UNIVERSITY OF READING
Department of Mathematics
Mathematical and Numerical Modelling of Atmosphere and Oceans MSc

A Moving Mesh Approach to Modelling the Grounding Line in Glaciology

Josie Dodd

August 2013

A dissertation submitted in partial ful lment of the requirement for the degree of Master of Science

Acknowledgements

Firstly I would like to thank my father, Paul Dodd whose love and generosity has made it possible to complete this course. Secondly I would like to thank my project supervisor Prof. Mike Baines for all of his patience and invaluable advice.

Contents

1 Introduction

Understanding the dynamics of marine ice sheets has been a subject of increasing

The glacier begins to float when there is enough water to support the weight of the ice. This is known as the condition for flotation and can be described by the equation

$$\rho_i h = \rho_w (l - b);$$

where ρ_i is the density of the ice, ρ_w is the density of sea water, h is the ice thickness, l is the sea level and b is the elevation of the ice base [11].

The position of the grounding line is dictated by its surrounding conditions and thus as the conditions change so too does the position of the grounding line.

The complexity of glacier dynamics is such that a purely analytical approach to modelling the grounding line is impossible. This gives rise to a distinct need for the use of numerical approximations to simulate the behaviour of the glacier. The use of computers and programming software is integral to this. The dynamics of grounding lines in glaciers has been closely examined in a variety of computational models where results are often inconsistent [2], with occasionally spurious projections methods of treating the coupling between the sheet and shelf and what continuity conditions are applied at the grounding line. Many models only examine the ice dynamics of the grounded ice sheet without the coupling of the oating ice shelf [11]. Hindmarsh, 1996 [3] suggests that it is possible to model the grounding line dynamics without any coupling between the sheet and the associated shelf. However, there are other models that examine the grounded ice sheet with the inclusion of coupling between the sheet and the ice shelf. The coupling can either involve full mechanical coupling betwen sheet and shelf using an ice stream model or a semi-coupling where only the ice ux through the grounding line is considered. This dissertation aims at examining the ice sheet with the inclusion of semi-coupling between the ice sheet and ice shelf.

Another contribution to the inconsistencies of the various models is their sensitivity to the resolution and the robustness of the numerical implementation. There are a number of methods that use xed grid techniques. These have a rigid unmoving structure and are by far the simplist to implement and best understood. These methods often stongly depend on the grid size, as features may exhibit sharp changes that can only be truly represented with a grid ne enough to capture them. The grounding line in particular is a feature that requires a ne resolution for reliable results. This, however, is computationally costly. An alternative method to gain higher resolution without the extensive computational cost is to consider adaptive mesh techniques. These techniques apply a ner mesh around the grounding line and allow a coarser resolution elsewhere, thus saving computational time. A third approach uses a moving mesh technique which allows the grid points (including the position of the grounding line) to be moved. Moving mesh techniques are considered more robust and reliable, as the grounding line is part of the solution and no interpolations are required [5]. The survey paper of Vieli and Payne [11] goes into detail of how the results di er between various numerical models with di erent numerical properties and we will make frequent references to this paper to compare our results.

1.3 The Governing Equations

Ice can be treated as an extremely viscous uid, which generally deforms under its own weight over a period of time, subject to mass gain and loss at the surface of the glacier due to snowfall or melting [7]. Generally the amount of accumulation (or snow) at the upper part of the glacier is greater than the amount of ablation (loss of mass through melting), and so the mass of this region is expected to increase over time. Further down the glacier near the shelf, the rate of accumulation is less than the rate of ablation and so the mass is expected to decrease in this region. If it is assumed that the ice spreads unidirectionally then ice will spread over the glacier as ice is pushed from the sheet towards the shelf. The total flux of ice between the sheet and the shelf is what we want to model in order to gain an idea about the behaviour of the grounding line.

It is convenient to make several assumptions in order to simplify the physical model. The key assumptions are as follows:

- The model uses the Shallow Ice Approximation, as defined below
- The bed is flat with no isostasy, (i.e. the ice sheet is not elevated or lowered in order to meet equilibrium with the Earths crust after change in mass.)
- Temperature and density are constant
- There is no basal sliding

The mass balance equation in the shallow ice approximation is taken to be [11]:

$$h_t + (hu)_x = m. \tag{1}$$

in the time dependent region $0 \leq x \leq b(t)$, where $x = 0$ is the fixed boundary at the ice divide (the top of the glacier), $b(t)$ is the moving boundary at the shelf front, $h(x,t)$ is the height of the ice sheet, $u(x,t)$ is the diffusive velocity, and $m(x)$ is the accumulation rate. The accumulation term represents the combination of mass gain from snow and mass loss from ablation.

The boundary conditions for this problem are that there is no flux at the fixed boundary $x = 0$ and so $u = 0$ at this point and also there is zero total flux at the moving boundary b(t). At the moving boundary $x = b(t)$ using Glen's flow law and the assumption of unidirectional flow the diffusive velocity u satisfies [11]

$$\left.\frac{\partial u}{\partial x}\right|_{b(t)} = A\left(\frac{1}{4}\rho_i g\left(1 - \frac{\rho_i}{\rho_w}\right)\right)^n h^n \tag{2}$$

where $h = h(b(t))$ and A is a constant known as the rate factor and is taken from Glen's flow law. Although the rate factor is dependent on the temperature of the ice (and in practice has a large impact in the speed of the ice flow), for the simplified model used in this dissertation we have taken it to be constant, its value being chosen as the value used in the EISMINT suite of test problems [11].

As the diffusive velocity $u(x,t)$ behaves very differently in the sheet and the shelf we split the problem into two sub-problems. Let $a(t)$ be the time dependent position of the grounding line, where $0 \leq a(t) \leq b(t)$. Then $x \in [0, a(t)]$ is the ice sheet region and $x \in [a(t), b(t)]$ is the ice shelf region.

1.3.1 The Ice Sheet

Using the physics of ice in the ice sheet region $0\,x \quad a$

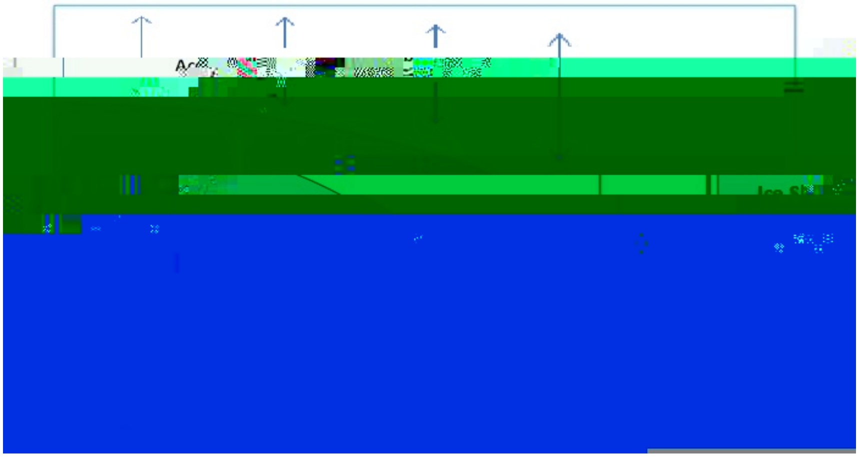

Figure 2: Illustration of Glacier

thickness of the ice below sea level to be equal to the sea level at the grounding line and so

$$l \quad \frac{i}{w} h_a = 0$$

where h_a is the the ice thickness at the grounding line. We can then calculate sea level by

$$l = \frac{i}{w} h_a:$$

In this wn0 16t-

In section 2 we investigate the behaviour of the diffusive velocity u in the sheet and shelf separately without the accumulation term m. We go on to discuss the numerical approximations used for both the sheet and shelf in section 2.3.

We then combine in section 3 the sheet and shelf calculations and the coupling between them. At this point an approach using conservation of mass fractions (CMF) is introduced. The mass fractions induce a deformation velocity v, which is generated by the diffusive velocity u and the coupling between the sheet and the shelf. This deformation velocity is then used to move the mesh. We are then able to recover the ice thickness algebraically using the local conservation principle. As this approach cannot be carried through analytically we need to find feasible ways to do it numerically. The numerical approximations for the deformation velocities and the recovery of the ice height using finite differences are also given in section 3. In section 4 we add the source term and outline the effect this has on the basic theory including the numerical algorithm.

In section 5 we discuss the non-dimensionalisation of the equations. In section 6 we use a test problem to investigate the significance of the viscosity of the ice and discuss a steady state solution. We go on to demonstrate the convergence of the moving mesh method used in this dissertation. We then go on to talk about the sensitivity of the model to various rates of accumulation in section 7.

In section 8 we introduce an elevation to the glacier bed. We discuss how this affects the model and also how the stability of the method is affected with varying gradients in the elevation. In section 9 we discuss the influence that changes in sea level has on the grounding line and finally in section 10 we investigate the influence that the rate factor A has on the evolution of the glacier.

Throughout sections 7 to 10 we compare results where appropriate, with the EISMINT test cases and the results in the Vieli and Payne survey paper [11].

To conclude we give a brief summary of our findings and discuss further work on improvements and generalisations.

2 Ice Di usion Only

leading to the alternative form of the nonlinear equation (9)

$$h_t = c\left(h\left(\frac{\partial h^{7/3}}{\partial x}\right)^3\right)_x \qquad (11)$$

for the change in thickness h in the ice sheet. It is equation (11) we have to solve for h in $(0; a(t))$ subject to the given boundary conditions.

2.2 Ice Shelf

The ice shelf covers the region $a(t) \leq x \leq b$

a moving mesh model. One of the ideas behind a moving mesh grid is to allow the grounding line to be followed continuously [11]. This approach is considered advantageous from a numerical point of view since the grounding line is part of the solution and no interpolation is needed [5]. Fixed grid models generally employ some interpolation, as the grounding line could be situated between two fixed grid points. In the survey paper of Vieli and Payne [11] it was found that fixed grid models are more dependent on numerical details such as grid size and so are not as robust as moving grid models [11]. The numerical scheme used in this dissertation adopts one particular moving mesh approach, which incorporates conserved mass fractions to move the mesh.

The domain $[0, b(t)]$ is divided into N intervals such that the initial spacing is constant, i.e. $\Delta x = b(0)/N$. As we are dealing with two separate domains we will use a subscripts 1 to denote the sheet and 2 for the shelf (e.g. N_1 for the sheet and N_2 for the shelf, where $N_1 + N_2 = N$). We will initially take equal intervals $\Delta x_1 = a(0)/N_1$ for the ice sheet and $\Delta x_2 = (b(0) - a(0))/N_2$ for the ice shelf, such that $x(j) = j\Delta x_1$ for $j = (0, \dots, N_1)$ is the distance along the ice sheet and $x(j) = j\Delta x_2$ for $j = (N_1, \dots, N_2)$ is the distance along the ice shelf. Subsequentially the intervals Δx_1 and Δx_2 will vary with time.

The diffusive velocity is approximated using finite difference schemes.

2.3.1 Ice Sheet

For the ice sheet a centred finite difference scheme is used at the interior points,

$$u_j = c\left(\frac{(h_{j+1})^{7/3} - (h_{j-1})^{7/3}}{x_{j+1} - x_{j-1}}\right)^3. \tag{15}$$

for $j = 1, \dots, N_1 - 1$. At $j = 0$ we use the fact that $\frac{dh}{dx} = 0$ and so $h_1 = h_{-1}$ which implies that $u_0 = 0$. At the boundary $x = a(t)$ a downwind scheme is used..

2.3.2 Ice Shelf

For the ice shelf we have two different approximations, firstly the approximation for a constant μ which gives us the linear elliptic equation given in (12) to solve, and secondly the approximation for a varying viscosity which gives the non-linear elliptic equation given in equation (14).

We approximate equation (12) using centred differences as follows:

$$\frac{2h_{j+1/2}\frac{u_{j+1}-u_j}{x_{j+1}-x_j} - 2h_{j-1/2}\frac{u_j-u_{j-1}}{x_j-x_{j-1}}}{x_{j+1/2}-x_{j-1/2}} = \mu^{-1} g h_j \frac{s_{j+1/2}-s_{j-1/2}}{x_{j+1/2}-x_{j-1/2}} \tag{16}$$

$j = N_1+1,\dots,N_2-1$. We use the midpoint average for half values h and s to get

$$(h_{j+1}+h_j)\left(\frac{u_{j+1}-u_j}{x_{j+1}-x_j}\right)-(h_j+h_{j-1})\left(\frac{u_j-u_{j-1}}{x_j-x_{j-1}}\right) = {}^{1} g h_j \frac{s_{j+1}-s_{j-1}}{2} \quad (17)$$

and so

$$\frac{h_j+h_{j-1}}{x_j-x_{j-1}}u_{j-1}-\left(\frac{h_{j+1}+h_j}{x_{j+1}-x_j}+\frac{h_j+h_{j-1}}{x_j-x_{j-1}}\right)u_j+\frac{h_{j+1}+h_j}{x_{j+1}-x_j}u_{j+1} = {}^{1} g h_j \frac{s_{j+1}-s_{j-1}}{2} \quad (18)$$

This can be written as a system of linear equations.

At the boundary $j = N_1$, u_0 is given. For the boundary at $x = b$ instead of a centred difference approximation we use a backward difference approximation

$$2h_j\left(\frac{\partial u}{\partial x}\right)_N - 2(h_N+h_{N-1})\left(\frac{u_N-u_{N-1}}{x_N-x_{N-1}}\right) = {}^{1} g h_N \frac{s_N-s_{N-1}}{2} \quad (19)$$

and use the boundary condition given in equation (2).

Thus the system of equation is given as

$$\begin{pmatrix}
\frac{h_2+h_1}{x_2-x_1}+\frac{h_1+h_0}{x_1-x_0} & \frac{h_2+h_1}{x_2-x_1} & & 0 \\
\frac{h_2+h_1}{x_2-x_1} & \frac{h_3+h_2}{x_3-x_2}+\frac{h_2+h_1}{x_2-x_1} & \frac{h_3+h_2}{x_3-x_2} & 0 \\
\vdots & \ddots & \ddots & \vdots \\
\vdots & \ddots & \ddots & \vdots \\
\vdots & \ddots & \ddots & \vdots \\
\vdots & \ddots & \ddots & \vdots \\
\vdots & \frac{h_{N-1}+h_{N-2}}{x_{N-1}-x_{N-2}} & \frac{h_N+h_{N-1}}{x_N-x_{N-1}}+\frac{h_{N-1}+h_{N-2}}{x_{N-1}-x_{N-2}} & \frac{h_N+h_{N-1}}{x_N-x_{N-1}} \\
0 & 0 & \frac{h_N+h_{N-1}}{x_N-x_{N-1}} & \frac{h_N+h_{N-1}}{x_N-x_{N-1}}
\end{pmatrix}
\begin{pmatrix} u_1 \\ u_2 \\ \vdots \\ \vdots \\ \vdots \\ \vdots \\ \vdots \\ \vdots \\ u_N \end{pmatrix}$$

$$= \begin{pmatrix}
{}^{1} g h_1 \frac{s_2-s_0}{2} - \frac{h_1+h_0}{x_1-x_0}u_0 \\
{}^{1} g h_2 \frac{s_3-s_1}{2} \\
\vdots \\
\vdots \\
\vdots \\
\vdots \\
\vdots \\
{}^{1} g h_N \frac{s_N-s_{N-1}}{2} - 2A\left(\frac{1}{4}\rho_i g\left(1-\frac{\rho_i}{\rho_w}\right)\right)^3 h_N^4
\end{pmatrix} \quad (20)$$

This is a tridiagonal system which we can solve for the diffusive shelf velocities u using Gaussian elimination.

For the non-linear elliptic equation with varying viscosity we employ a different method to approximate the diffusive velocity u. For this we will use Picard iteration. This is a simple first order iteration method. Given the equation

$$2\frac{\partial}{\partial x}\left[h\left(\frac{\partial u}{\partial x}\right)^{1/3}\right] = A^{1/3}\, g h\frac{\partial s}{\partial x}$$

from section 2.2, a finite difference scheme will give us the following approximation

$$\frac{2h_{j+1/2}\left(\frac{u_{j+1}-u_j}{x_{j+1}-x_j}\right)^{1/3} - 2h_{j-1/2}\left(\frac{u_j-u_{j-1}}{x_j-x_{j-1}}\right)^{1/3}}{x_{j+1/2}-x_{j-1/2}} = A^{1/3}\, g h_j \frac{s_{j+1/2}-s_{j-1/2}}{x_{j+1/2}-x_{j-1/2}} \tag{21}$$

We are able to use the midpoint average for half values h and s to get

$$(h_{j+1}+h_j)\left(\frac{u_{j+1}-u_j}{x_{j+1}-x_j}\right)^{1/3} - (h_j+h_{j-1})\left(\frac{u_j-u_{j-1}}{x_j-x_{j-1}}\right)^{1/3} = A^{1/3}\, g h_j \frac{s_{j+1}-s_{j-1}}{2} \tag{22}$$

So u_j satisfies the nonlinear system

$$(h_{j+1}+h_j)\left(\frac{u_{j+1}-u_j}{x_{j+1}-x_j}\right)^{1/3} - (h_j+h_{j-1})\left(\frac{u_j-u_{j-1}}{x_j-x_{j-1}}\right)^{1/3} - A^{1/3}\, g h_j \frac{s_{j+1}-s_{j-1}}{2} = 0 \tag{23}$$

for $j = N_1+1, \ldots, N_2-1$.

For the boundary at $j = N_2$ instead of a centred difference approximation we will use a backwards difference approximation

$$h_j\left(\frac{\partial u}{\partial x}\right)_b^{1/3} - (h_j+h_{j-1})\left(\frac{u_j-u_{j-1}}{x_j-x_{j-1}}\right)^{1/3} - A^{1/3}\, g h_j \frac{s_{j+1}-s_{j-1}}{2} = 0 \tag{24}$$

and apply the boundary condition described in equation (2). At $x = a(t)$ we will also use the given diffusive velocity u. We now have the following system of non linear equations

$$F(u) = \left(\begin{array}{l} (h_2+h_1)\left(\frac{u_2-u_1}{x_2-x_1}\right)^{1/3} - (h_2+h_a)\left(\frac{u_1-u_a}{x_1-x_a}\right)^{1/3} - A^{1/3}\, g h_1 \, s_2 - s_a \\ \vdots \end{array}\right.$$

method,

$$u^{new} = u^{old} \quad F(u^{old})$$

we can nd the di usive velocity of the ice shelf provided that the iterations converge.

moving mesh methods where a purely geometrical criterion is often employed. In such methods the moving domain $x \in [0, b(t)]$ is mapped to a fixed domain $\xi \in [0, 1]$ by the transformation $\xi = \frac{x}{b(t)}$; $\tau = t$. Using the chain rule to differentiate $h(\xi, \tau)$ with respect to ξ and τ transforms (1) into

$$\frac{\partial h}{\partial t} - \frac{\xi}{b(\tau)} \frac{\partial b(\tau)}{\partial \tau} + \frac{\partial (hu)}{\partial \xi} = m \tag{31}$$

Note that this approach adds another term to the left hand side that is not a total derivative with respect to ξ and therefore the equation is no longer in divergent form. This feature can lead to unphysical effects in the method, such as not being mass conserving when $m = 0$.

system is one. Observe that $c_1(0;a) = 1$ and $c_2(a;b) = 1$. When held constant these mass ratios can be used to induce modified velocities.

3.2 Deformation Velocities

We shall move the points $x(t)$ such that the mass fractions in equation (34) will remain constant over time, which we can do even with a non-zero flux between the ice sheet and shelf.

Whereas in equation (27) we could have written $\int_0^{x(t)} h_1(x;t)dx = c(0;x)$, we now have, from equation (34), that $\int_0^{x(t)} h_1 dx = {}_1 c(0;x)$ and so

$$\frac{d}{dt}\int_0^{x(t)} h_1 dx = -_1 c_1(0;x) \tag{35}$$

and similarly

$$\frac{d}{dt}\int_{x(t)}^{b(t)} h_2 dx = -_2 c_2(x;b). \tag{36}$$

Using Leibnitz Rule, we find that

$$\frac{d}{dt}\int_0^{x(t)} h_1 dx = \int_0^{x(t)} \frac{\partial h_1}{\partial t} dx + [hv]_0^{x(t)} \tag{37}$$

where $v = \frac{dx}{dt}$ is the modified velocity which is induced by the mass fractions. We can substitute for $\frac{\partial h_1}{\partial t}$ from the mass balance equation (8) to get

$$\begin{aligned}\frac{d}{dt}\int_0^{x(t)} h_1 dx &= \int_0^{x(t)} (\ (h_1 u_1)_x + (h_1 v_1)_x)\, dx \\ &= [h_1(\ u_1 + v_1)]_0^{x(t)} \\ &= h_1(x)(\ u_1(x) + v_1(x))\end{aligned} \tag{38}$$

since $v_1(0) = u_1(0) = 0$. Hence

$$h_1(x)(\ u_1(x) + v_1(x)) = -_1 c_1(0;x)$$

giving

$$v_1(x) = u_1(x) + \frac{-_1 c_1(0;x)}{h_1(x)} \tag{39}$$

by equation (35).

Similarly

$$\frac{d}{dt}\int_{x(t)}^{b(t)} h_2 dx = \int_{x(t)}^{b(t)} (\quad (h_2u_2)_x + (h_2v_2)_x)\, dx$$
$$= [h_2(\quad u_2 + v_2)]_{x(t)}^{b(t)}$$

$$\frac{d}{dt}\int_{x(t)}^{b(t)} h_2 dx = h_2(b)(\quad u_2(b) + v_2(b)) \quad h_2(x)(\quad u_2(x) + v_2(x)): \tag{40}$$

Hence

$$h_2(b)(\quad u_2(b) + v_2(b)) \quad h_2(x)(\quad u_2(x) + v_2(x)) = -_2 c_2(x; b)$$

by equation (36). As we have zero ux at the boundary $x = b$, then $h_2(b)(\quad u_2(b) + v_2(b)) = 0\,; \quad 8h_2(b)$ and so $v_2(b) = u_2(b)$. Therefore

$$v_2(x) = u_2(x) \quad \frac{-_2 c_2(x; b)}{h_2(x)}: \tag{41}$$

Putting $x = a$ into equations (39) and (41) gives us that $-_1 = h_a(\quad u_a + v_a) = \quad -_2$

3.3.1 Time Stepping

Once we have the approximation v_a substituted into equations (42) and (43) we get the velocities of the moving points. We now move each grid point with its corresponding velocity, doing this in the same way as in section 3.3 equation (26). However instead of u_j, we now use v_j. Since λ_1 and λ_2 vary over time we must also find their new values after each time step. As in equation (26) these are calculated using the explict Euler scheme as follows:

$$\lambda_1^{n+1} = \lambda_1^n + \Delta t\,\dot{\lambda}_1; \qquad \lambda_2^{n+1} = \lambda_2^n + \Delta t\,\dot{\lambda}_2 \tag{44}$$

3.3.2 Recovering h

All that is left is to calculate the new ice heights. From equation (34) we can deduce that:

$$\frac{1}{\lambda_1}\int_{x_{j-1}}^{x_{j+1}} h_1 dx = c_{1;j+1} - c_{1;j-1} \quad \text{and} \quad \frac{1}{\lambda_2}\int_{x_{j-1}}^{x_{j+1}} h_2 dx = c_{2;j-1} - c_{2;j+1}$$

Note that for the ice shelf c_j gets smaller as we progress along the shelf and so we subtract c_{j+1} from c_{j-1} to achieve the same effect as for the ice sheet. Using the new values of λ_1 and λ_2 found in section 3.3.1 we find the new mass of ice between x_{j-1} and x_{j+1} by

$$\int_{x_{j-1}}^{x_{j+1}} h_1 dx = \lambda_1[c_{1;j+1} - c_{1;j-1}] \quad \text{and} \quad \int_{x_{j-1}}^{x_{j+1}} h_2 dx = \lambda_2[c_{2;j-1} - c_{2;j+1}] \tag{45}$$

Approximating the integrals by the midpoint rule again we can retrieve the new values for the ice heights as follows:

$$h_j = \frac{\lambda_1(c_{1;j+1} - c_{1;j-1})}{x_{j+1} - x_{j-1}}; \qquad h_j = \frac{\lambda_2(c_{2;j-1} - c_{2;j+1})}{x_{j+1} - x_{j-1}} \tag{46}$$

2. Calculate the mass fractions $c_1(0; x_j)$ for $j \in [0; \ldots; N-1$

4 Adding the Source Term

Up until now we have only considered the problem where the accumulation is zero. This is unrealistic as we would usually expect either snow or melting to change the total mass. To incorporate this we will now reintroduce the accumulation term $m(x)$ back into the equations and investigate how this will a ect the algorithm. The function m is independent of time and will initially be taken as a constant to simulate

$$v_1(x) = u_1(x) + \frac{\left(h_a(-u_a + v_a) + \int_0^{a(t)} m\,dx\right)c_1(0;x) - \int_0^{x(t)} m\,dx}{h_1(x)} \tag{54}$$

$$v_2(x) = u_2(x) + \frac{\left(h_a(-u_a + v_a) - \int_{a(t)}^{b(t)} m\,dx\right)c_2(0;x) + \int_{x(t)}^{b(t)} m\,dx}{h_2(x)} \tag{55}$$

The grounding line migration rate is now the same as in equation 6 reproduced here for convenience,

$$v_a = \frac{-\frac{\rho_w}{\rho_i}\frac{\partial f}{\partial t} + \frac{\partial (hu)}{\partial x} - m(x)}{\frac{\partial h}{\partial x} - \frac{\rho_w}{\rho_i}\frac{\partial f}{\partial x}}.$$

Letting a denote the grid point for the grounding line we can approximate the migration rate by

$$v_a = \frac{-\frac{\rho_w}{\rho_i}\frac{f^n - f^{n-1}}{\Delta t} + \frac{(hu)_{a+1} - (hu)_{a-1}}{x_{a+1} - x_{a-1}} - m_a}{\frac{h_{a+1} - h_{a-1}}{x_{a+1} - x_{a-1}} - \frac{\rho_w}{\rho_i}\frac{f_{a+1} - f_{a-1}}{x_{a+1} - x_{a-1}}}.$$

where the superfixes n and $n-1$ represent the time levels.

Note that we update the grid points positions, θ_1 and θ_2 in the same way as in section 3 using the explicit Euler method in equations (26) and (44). All that is left is to recover the new ice heights from the mass constants as in equation (46). For convenience we will summarise the algorithm for the added accumulation term:

1. Compute θ_1 and θ_2 in the inital profile by integrating h with respect to x between $(0; a(t))$ and $(a(t); b(t))$ respectively.

2. Calculate the mass fractions $c_1(0; x_j)$ for $j \in [0; \ldots; N^1]$ and $c_2(x_j; b)$ for $j \in [N^1; \ldots; N^2]$ by integrating h with respect to x between $(0; x_j)$ for $j \in [0; \ldots; N^1]$ and $(x_j; b(t))$ for $j \in [N^1; \ldots; N^2]$ respectively.

   For each time step:

3. Calculate the deformation velocities using equations (54) and (55).

4. Move the grid nodes with the calculated velocities using the explicit Euler method.

5. Find the new values for θ_1 and θ_2 using the expicit Euler method.

6. Use the new values of θ_1 and θ_2 to find the new values for the mass fractions using equation (45).

7. Retrieve the new values of the ice height h_j from equation (46) using the mid-point rule and the new mass fractions.

5 Non-Dimensionalisation

In order to compare with real data we proceed to make this model non-dimensional. Non-diminsionalisation is accomplished by dividing each variable by a constant scaling parameter. Suppose we scale h, u, x, t, and m so that

$$h = \frac{h}{[h]}; \quad x = \frac{x}{[x]}; \quad t = \frac{t}{[t]}; \quad u = \frac{u}{[u]}; \quad m = \frac{m}{[m]}$$

where the square brackets indicate the corresponding scaling parameter and the super x represents the scaled variable.

From equation (1) we find that the scaled shallow ice equation becomes

$$\frac{[h]}{[t]} h^x_x + \frac{[h]}{[x]}[u](h\ u\ )_x = [m]m\ :$$

For balance to be maintained within equation (1) we must have

$$\frac{[h]}{[t]} = \frac{[h]}{[x]}[u] = [m]; \quad \text{so} \quad [t] = \frac{[x]}{[u]}; \quad \text{and} \quad [m] = \frac{[h]}{[x]}[u]$$

5.1 Sheet

Using the diffusive velocity equation for the sheet given in section 2.1 as

$$u = c \quad \frac{\partial h^{7/3}}{\partial x}^{3}$$

we obtain the scaled ice diffusion velocity u

$$[u]u = [c]\frac{[h]^7}{[x]^3}c \quad \frac{\partial (h\ )^{7/3}}{\partial x}^{3}$$

where

$$c = \frac{c}{[c]}$$

Again we must ensure that both sides are balanced and so

$$[u] = [c]\frac{[h]^7}{[x]^3}$$

5.2 Shelf

In the shelf we have a di erential equation for ice di usion velocity repeated here for convenience,

$$2(\; hu_x)_x = \;\; ghs_x:$$

In the case where is variable, given as $= A \;\; ^{1=3}(u_x) \;\; ^{2=3}$, the di usive velocity in the ice shelf satis es

$$2(h(u_x)^{1=3})_x = A^{1=3} \; g\, h(s_x): \tag{56}$$

The constant c used in the sheet calculations is given by

$$c = \frac{3}{7} \;\; ^3 \frac{2A \;\; ^3 g^3}{5}$$

Using this in equation (56) gives

$$2(h(u_x)^{1=3})_x = \frac{7}{3} \;\; ^3 \frac{5c}{2} \; ! \; ^{1=3} \; h\, s_x:$$

Therefore the scaled expression for the shelf velocity is given by

$2x$

xx ^{3} 5

$b\, s$

5s-3267(th)-9.2726(s)-6

6 A 1D Test Case

Following the EISMINT test case [11] we consider a glacier where both the ice sheet and ice shelf have an initial length of $50km$. We also need an initial profile for the ice thickness; this has been chosen to be

$$h = (1 - 0.75x^2)^{3/7}; \qquad x \in (0, 1) \tag{57}$$

which is similar to the initial profile chosen in [4]. Table 1 shows a summary of the parameters used in the model.

Value	Physical Parameter
n = 3	

Running the model with zero accumulation exhibits negligible change to the initial conditions, with the change to the grounding line position becoming less than $0.1 ma^{-1}$ within 2 years. We might ask why the larger mass of the ice at the ice divide does not distribute itself along the domain over time. A glacier flows in the direction of decreasing surface elevation. As the shelf is buoyed by the ocean the surface elevation changes only marginally and so the flow is relatively small.

The inability of this model to reach a non-arbitary steady state is worrying as this is significantly different to the results found in previous studies. The potential cause of this inability to reach steady state is choosing a constant accumulation across the glacier. Since the method conserves mass, a constant source term will not allow a steady state solution as there is no flux of mass out of the system. This implies that instead of the constant accumulation term given in the Vieli and Payne [11] paper it is better to represent the accumulation with a linear equation. We will let

$$(1 \quad x)$$

represent the accumulation profile, where is a parameter used to control the scale of the accumulation and determines where the source term changes from accumulation to ablation. If we choose and such that

$$\int_0^{b(t)} m\,dx = 0.3 ma^{-1}$$

then we find the initial ice profile meets the requirements of a steady state described in the MISMIP [5] papers with negligible change to the initial conditions (i.e. the change in grounding line position is less than $0.1 ma^{-1}$ and the change in ice thickness is less than $1 ma^{-1}$).

6.2 Viscosity

We are interested in the effect of simplifying the model, so viscosity is left as a constant. We ran the model with $\int_0^{b(t)} m(x)dx = 0.5 ma^{-1}$ for varying N for 5000 years. Note that for a net accumulation of $0.5 ma^{-1}$ we have chosen $= 0.0002$ and $= \frac{3}{2}$. The approximations set out in the equations (20) and (25) have been used, one in the case of constant viscosity and the other using varying viscosity. The results are displayed in table 2 and table 3, with the relative differences shown in table 4. The difference in grounding line position (GLP) between the the two methods is very small, although it becomes slightly larger with increased resolution. Also the change in shelf front position differs between the two methods, the shelf front receding with the varying viscosity and advancing with the constant viscosity, although the difference decreases with an increased resolution.

N	t	GLP	Shelf Front	h at GLP
11	0.01	50.249357	100.0000008	914.502872
21	0.25	50.400903	100.0000007	915.532212
41	0.0625	50.429636	100.0000008	915.721627
81	0.015625	50.432728	100.0000008	915.740688

Table 2: Table of Values for Constant Viscosity

N	t	GLP (km)	Shelf Front (km)	h at GLP (m)
11	0.01	50.252652	99.998139	914.511045
21	0.25	50.404234	99.998295	915.539494
41	0.0625	50.433251	99.998381	915.728938
81	0.015625	50.436981	99.998427	915.748842

Table 3: Table of Values for Varying Viscosity

N	t	GLP	Shelf Front	h at GLP
11	0.01	0.0065575%	0.0018616%	0.0008936%
21	0.0025	0.0066089%	0.0017057%	0.0007952%
41	0.000625	0.0071676%	0.0016193%	0.0007983%
81	0.00015625	0.0084320%	0.0015739%	0.0008904%

Table 4: Table of Relative Differences between Varying and Constant Viscosity

Although the differences are very small, constant viscosity is regarded as too crude an assumption to make and, as incorporating the varying viscosity is relatively simple, all future experiments viscosity will be taken as the variable case,

$$= A^{1/3}\left(\frac{\partial u}{\partial x}\right)^{2/3}.$$

6.3 Convergence

To decide if this numerical scheme is a useful tool in predicting the evolution of grounding lines we must show that the method is convergent. The position of the grounding line for a series of increasing values of N and a decreasing series of values of t has been recorded in table 5. To maintain stability t has been chosen such that $t \propto N^{2}$. Variable viscosity has been included and the accumulation rate has been taken to be $\int_0^{b(t)} m(x)dx = 0.5 m a^{1}$. The final time has been set relatively low at 2500 years. This has been chosen because running the model for long time periods with a very fine resolution is computationally costly.

We now need to calculate the errors. As we do not have an exact solution or any comparable raw data the value for the grounding line position with the finest

N	t	Position of Grounding Line	Ice Height
11	0.01	50.014602	913.835880
21	0.25	50.178554	914.982169
41	0.0625	50.215269	915.234004
81	0.015625	50.222920	915.285344
161	0.00390625	50.224352	915.293350
321	0.0009765625	50.224840	915.293729

Table 5: Table of Values

value are fine enough to closely resemble to the 'exact' solution, this would imply that this value is misleading.

6.4 Velocity

The velocity of each grid point for two accumulation profiles has been plotted in figure 3. The solid lines show the velocity for a positive net accumulation of $\int b(t)$

size and also a strong tendency for the grounding line to advance. In contrast to this there is no bias for the grounding line to advance or retreat for the moving mesh techniques of the Vieli and Payne paper. In addition, the difference in grounding line position between different numbers of grid nodes is much smaller for the moving mesh methods.

For our model there is some dependency of grounding line position on the number of grid points, however this is smaller than the initial x. Table 6 shows us that there is less than half a percent difference in grounding line position between a coarser grid and a finer grid, which amounts to approximately 200m. This is less than the initial grid spacing and therefore in the resolution of the model. This shows us that the dependency on the number of grid points is small.

Table 5 shows that the change in grounding line position increases with increased N. This is contrary to the results of the Vieli and Payne survey paper [11]. Another difference between the moving mesh method of this dissertation and the ones used in the Vieli and Payne paper is that the tendency of the grounding line is dictated by the sign of the accumulation. For a positive net accumulation the grounding line will advance and for a negative accumulation the grounding line will recede. Whereas the grounding line in the Vieli and Payne paper models will recede for small positive values of accumulation.

7 Changes to the Accumulation Rate

For a positive net accumulation we expect the grounding line to advance and for a negative net accumulation we expect the grounding line to recede. For an increased magnitude in accumulation we would expect to see an increase in the change of grounding line position. The ice thickness profiles for different accumulation rates are shown in figure 4. Note that $= 0.0002$ and is given various values with $= \frac{3}{2}$ corresponding to a net accumulation of $0.5ma^{-1}$, $= \frac{19}{10}$ corresponding to a net accumulation of $0.1ma^{-1}$, $= \frac{21}{10}$ corresponding to a net accumulation of $0.1ma^{-1}$ and $= \frac{5}{2}$ corresponding to a net accumulation of $0.5ma^{-1}$. The final time is $15ka$. There are 21 horizontal grid points for these plots and t has been taken to be 0.0025.

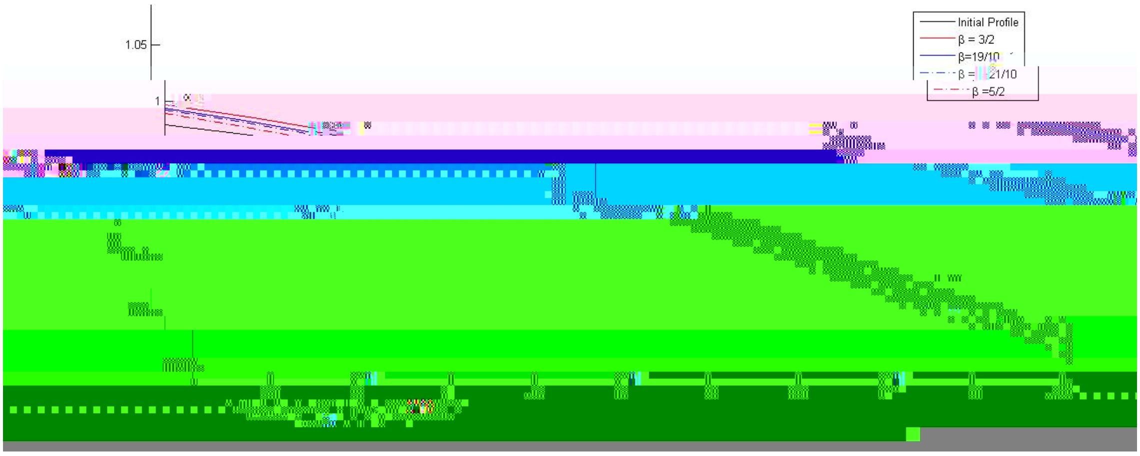

Figure 4: Ice thickness profile after 15000 years for different values of . The crosses mark the grounding line position.

The expectations of the changes to the grounding line position with different accumulation rates have been met here. There is one key difference between the moving mesh method of this dissertation and those discribed in the Vieli and Payne survey paper. There are some cases in the Vieli and Payne paper that for even a positive accumulation there is still a retreat in the grounding line position. This is counter intuitive as a positive accumulation would indicate that there is mass gain. If the mass increases around the grounding line then it would require more water to bouy the mass of the ice. If the sea level remains constant then there will not be enough water to bouy the ice just ahead of the grounding line and so the flotation criterion will no longer be met. Thus the grounding line will advance. The fact that

8 Introducing a Tilt

Up until now we have only discussed a glacier with a at bed but in reality this is not the case. In order to make the model more realistic we now incorporate an elevation to the ice bed. This will change the way in which we treat the di usive velocity set out earlier in equation (3). We previously stated that, in the sheet $s = h$

that the grounding line positions in moving mesh models are independent of basal slope. With such a varying field of conclusions and results it is still uncertain how the basal slope should affect the grounding line position.

We are interested in observing the impact of bed elevation on the migration of the grounding line for this moving mesh model. The model has been run for each glacier profile from figure 6 for a final time of 15000 years with $\int_0^{b(t)} m(x)dx = 0.5ma^{-1}$. and with $\int_0^{b(t)} m(x)dx = -0.5ma^{-1}$. There are 21 grid points, and $dt = 0.0025$. There is less than a 200m difference in grounding line position between the basal slopes for either an advance or a retreat. For the upsloping bed the grounding line will advance more compared to the flat and downsloping bed and retreat the least. The downsloping bed will retreat by the largest amount but advance by the smallest amount compared to the flat and upsloping bed.

There doesn't appear to be any change in tendency of grid point evolution with the varying beds and the difference in grounding line position for different basal slopes is smaller than the initial grid size and so within the accuracy of the model, indicating that the model is independent of basal topography. This agrees with the results found in the Vieli and Payne survey paper [11] and the results of Hindmarsh [3].

proLking more geinininini-410lin andw-3intidininoundicebasarasnininінthe vsheet314(the6)stat

gure 8. When the grounding line advances the ice thickness decreases, however for an upsloping bed we still see that the ux has the largest magnitude. Again, this indicates that the ux is dominated by the large velocity at the grounding line.

The reason for the larger uxes for the upsloping bed is due to the large grounding line velocities. The f_x term now incorporates b_x in the new formula (59) for grounding line migration (59). For an upsloping bed this has the opposite sign to the downward sloping bed, the result of which is that the denominator of the grounding line migration equation is now much smaller and hence the grounding line migration is much larger.

The grounding line position has been plotted in gure 9 for all three basal slopes using the new grounding line migration rate. The nal time is 15000 years, there are 21 grid points, and $t = 0:$

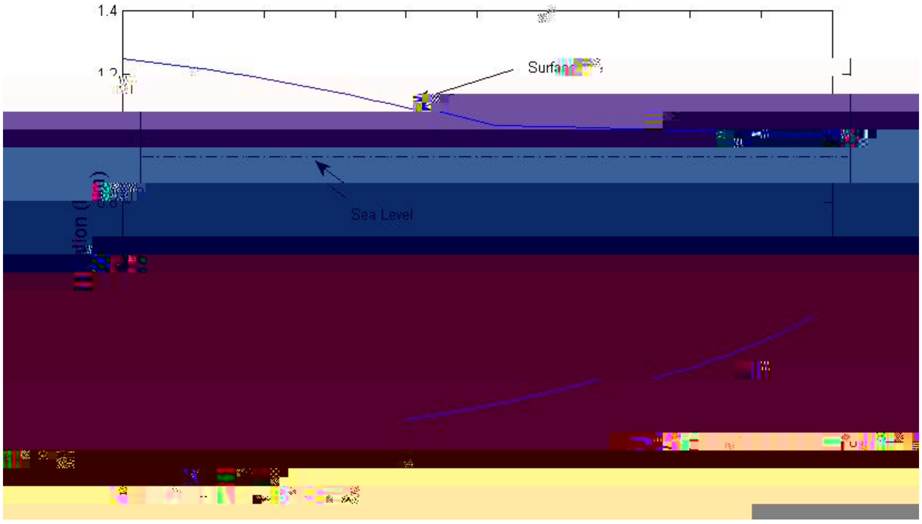

(a) Downward Slope

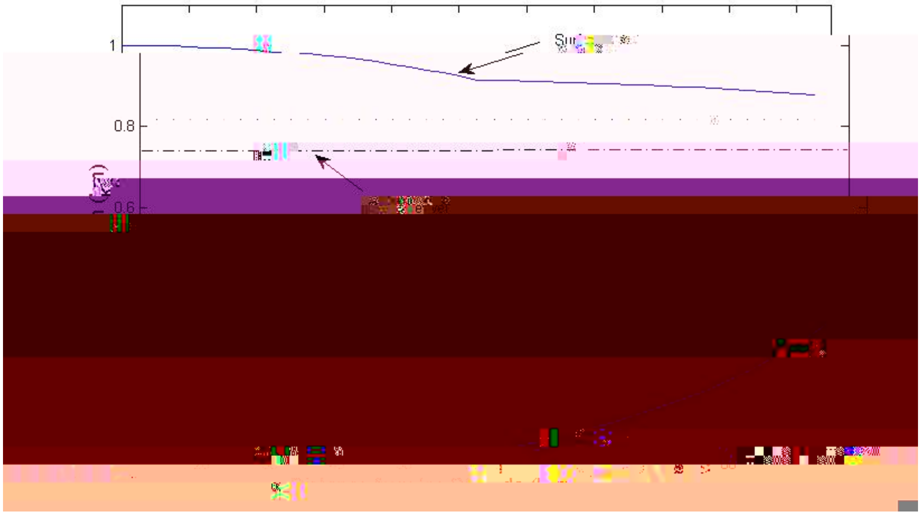

(b) Flat Bed

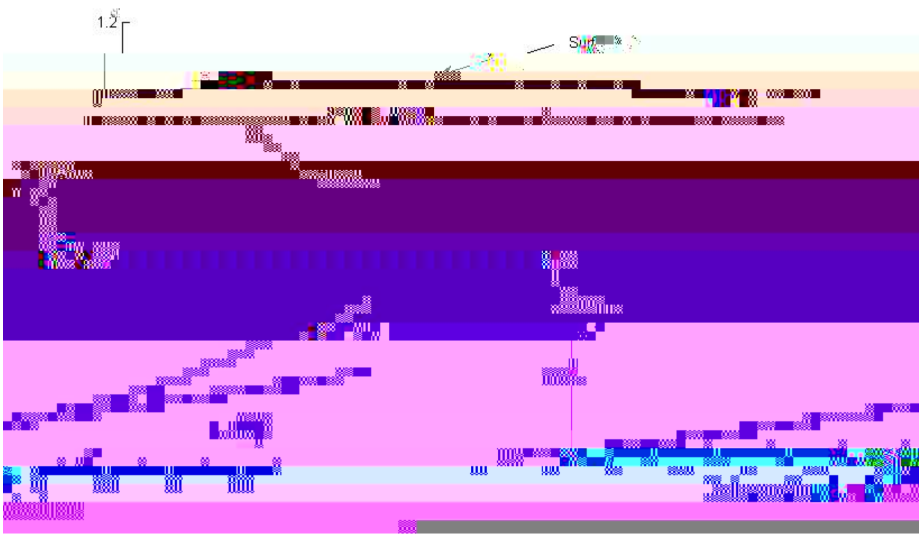

(c) Upward Slope

Figure 6: Di erent Ice Bed Pro les

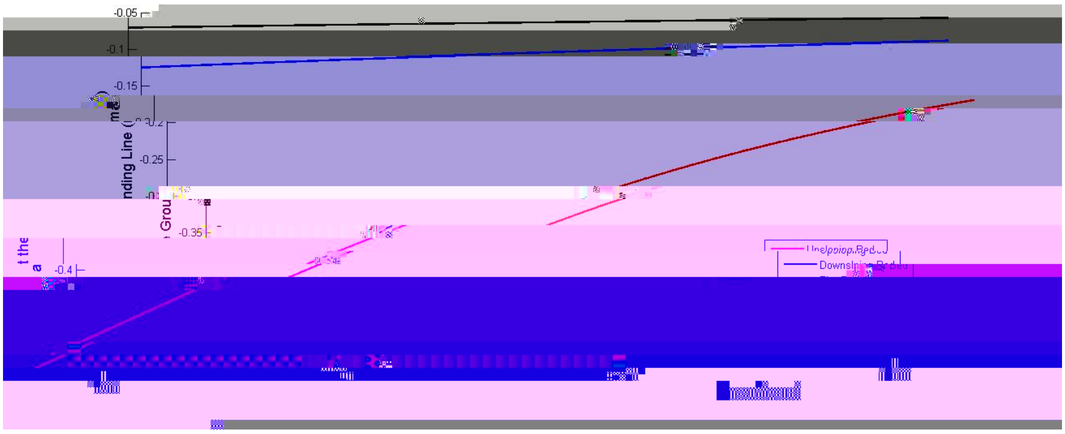

Figure 7: Flux at the Grounding Line for each basal slope with $\int_0^{b(t)} m\,dx = -0.5\,\mathrm{m\,a}^{-1}$

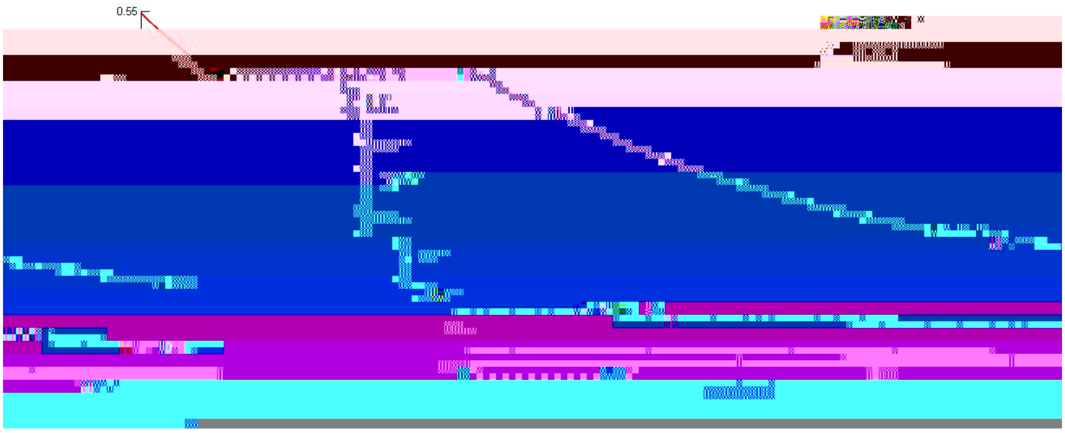

Figure 8: Flux at the Grounding Line for each basal slope with $\int_0^{b(t)} m\,dx = 0.5\,\mathrm{m\,a}^{-1}$

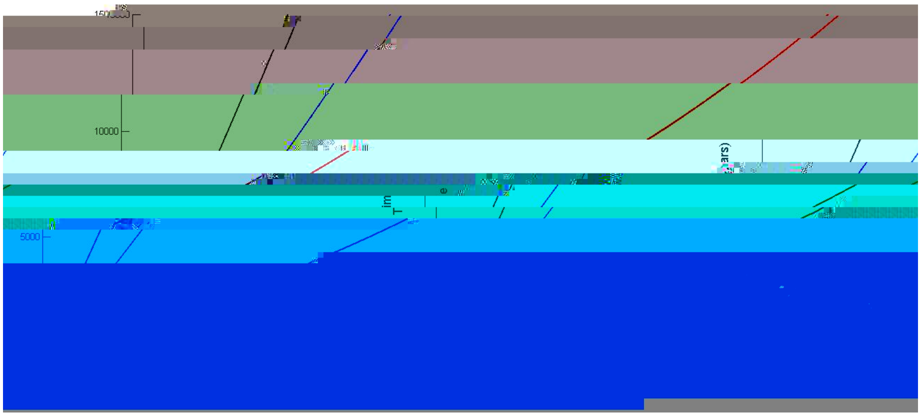

(a) Advancing Glacier

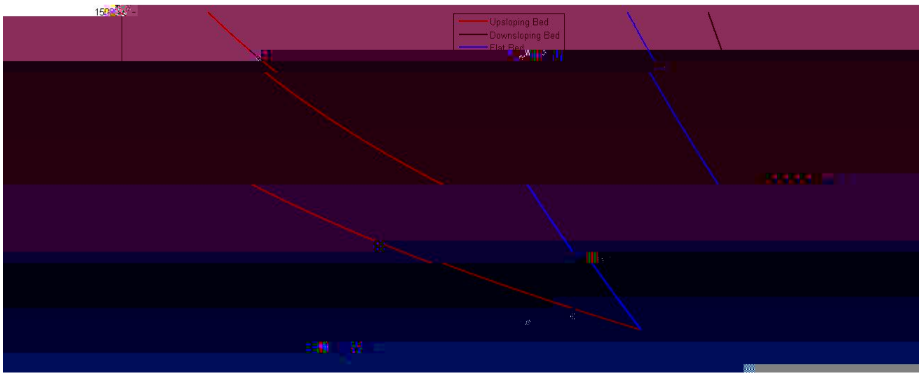

(b) Receding Glacier

Figure 9: The grounding line position over 15000 years for di erent basal slopes

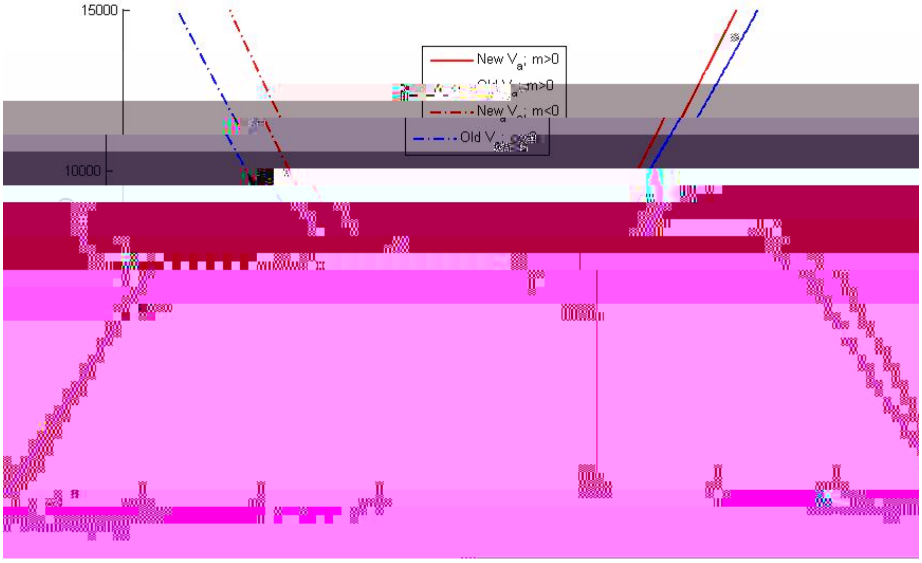

(a) Downward Slope

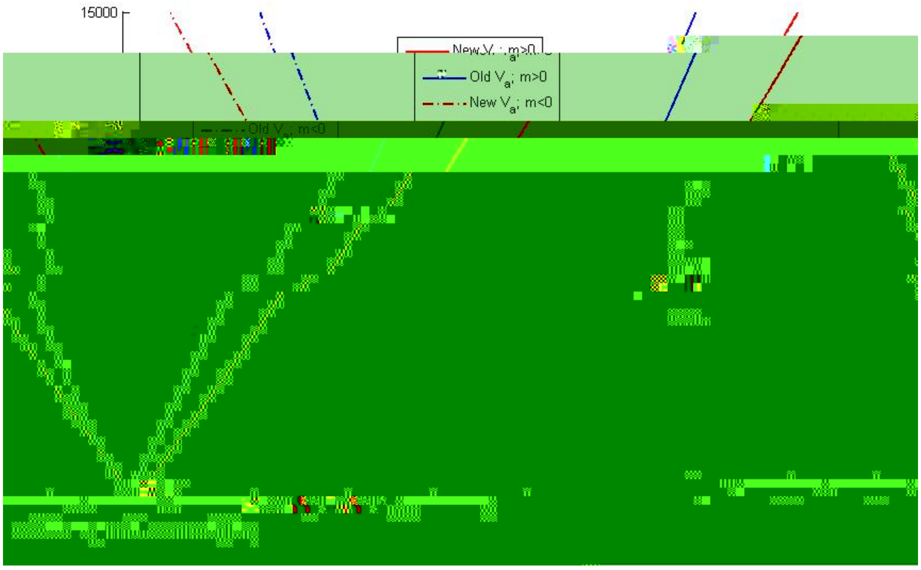

(b) Flat Bed

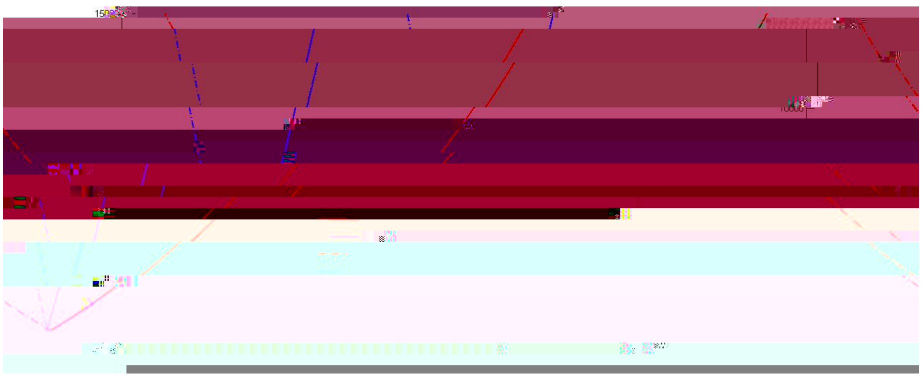

(c) Upward Slope

Figure 10: Comparison of the change in grounding line postion between the new and old equation

9 Changes to Sea Level

We allow the sea level to change by 5% over 1000 years, which amounts to a change of approxiately $60m$. For this experiment there are 21 grid nodes and t is set to 0.000625, the net accumulation is set to $\int_0^{b(t)} m(x)dx = 0.3ma^{-1}$, which allows the initial profile to remain in approximate steady state. For a sea level rise of 5% the grounding line recedes by approximately $3.8km$. For a 5% decrease in sea level the grounding line advances by appoximately $7.5km$. This is a much larger change than that described by the moving mesh models in the Vieli and Payne survey paper, where the grounding line position recedes by approximately $2km$ for a of sea level rise of $125m$ and advances by $1.5km$ for a decrease of sea level of $125m$. The grounding line migration of this method is also larger than the migration of the fixed grid methods of the Vieli and Payne paper. These differences could be attributed to the difference in the initial profile. For this dissertation we chose the sea level such that the flotation criterion was met at the mid point of the glacier. This is counter-intuitive as sea level determines the position of the grouning line and not vice versa. We chose this way as we wanted to replicate the conditions in the EISMINT experiments. Instead, if we allow the sea level to be $500m$ and obtain the expected position of the grounding line using the flotation criterion, we find that the resulting values for the migration of the grounding line are very different. Allowing the same changes to sea level as before gives an advance of less than $1km$ $.5km$ grounding factor had very little e ect on the grounding line dynamics although the absolute values in grounding line change were larger [11]. For the moving mesh method of this dissertation a higher rate factor makes very little change to the grounding line. In an advancing glacier the di erence in grounding line position is marginally larger for a higher rate factor. For a receding glacier the change in grounding line position is marginally smaller for the higher rate factor.

This indicates that this model is not very sensitive to the ice rheology; similar to the Vieli and Payne paper. This indicates that errors in the modelled ice temperature will not strongly a ect the results.

11 Conclusion and Discussion

Accurate and e cient modelling of the grounding line in glaciology is crucial in order to make reliable forcasts of the fate of the Cryosphere. Changes to grounded ice in the Cryosphere will greatly impact upon the Earth's climate system. Recent rates of receding ice sheets has prompted an increase in the desire to properly understand the dynamics of these glaciers. The modelling of glacier dynamics has experienced considerable development in recent years. However the results thus far have been inconsistent.

One common feature in many recent studies, such as the MISMIP [5] and Vieli and Payne [11] survey papers is that moving mesh models are often more reliable

Section 3.3.3 outlined an algorithm for the method so far.

We then went on to discuss how we recover the new ice heights using mid-point approximations, made possible by the conserved mass fractions method.

We reintroduced the accumulation term in section 4 and discussed how this affected the algorithm in section 3.3.3.

In section 5 we discussed the necessity of non-dimensionalisation for application to real data and how we facilitated this necessity in the method.

Section 6.1 investigated the steady state solution and found that our model achieves a near steady state, where h_ξ is sufficiently small, when the accumulation term is sufficiently small.

Section 6.2 investigated how the viscosity affected the model and found that the difference between varying and constant viscosity is relatively small, however it does alter the tendency of the shelf front to advance or recede. Despite the very small difference in varying viscosity and constant viscosity, incorporating the varying viscosity is relatively easy and so it is preferable to include it, as constant viscosity is too crude an assumption to make.

We tested for convergence in section 6.3 and showed that our method is convergent and approximately second order.

We examined the dependency of the model on the number of nodes in section 6.5. We found that the method is reliable with a coarse resolution, as the method is not stongly reliant on the number of nodes. This demonstrated a robustness typical of moving mesh models.

Section 7 investigated how changes to the accumulation affected the evolution of the glacier. We found that changes to the accumulation rate caused the glacier to evolve in a way that we would expect. For example, a positive accumulation caused the grounding line to advance and a negative accumulation caused the grounding line to recede. For a net accumulation of zero the grounding line position hardly changed. We also found that changes to the glacier incurred by changes in the accumulation were reversable. We found that the model is strongly dependent on the chosen accumulation rate, which is problematic as modelling the accumulation and ablation measurements can be inaccurate and that the CMF moving mesh method is stable for all basal slopes. However the the grounding line migration is dependent on basal topography.

Section 9 investigated how the model reacts to changes to in sea level and found that changes in sea level a ected the grounding line position in a way we would expect. For example a rise in sea level caused the grounding line to recede and a decrease in sea level caused the grounding line to advance. We also found that changes to the grounding line position incurred by changes in sea level were reversable.

Finally, section 10 investigated how changes to Rate Factor A a ected the model and the sensitivity of the model to ice temperature. We found that the model was not highly dependent on the rate factor and therefore insensitive to the modelled ice temperature.

The main aims of this dissertation have been to investigate the e ciency of the CMF moving mesh approach at modelling the migration of the grounding line and investigate how the behaviour of this model correlates with other schemes. We found that the model is convergent and we have been able to make favourable comparisons to the moving mesh models discussed in the Vieli and Payne survey paper [11], however our model does exhibit several distinct di erences.

to include these factors may change the results.

To conclude, this dissertation is unique in the sense that we have used a moving mesh method based on conserved mass fractions with the addition of semi-coupling between the sheet and shelf. Dale Partridge [4] used the same moving mesh method for a grounded ice sheet without the addition of the semi-coupling between the sheet and the shelf. To have an increasing ice height for a receding glacier on an upward slope, an amendment to the otation criterion described in the Vieli and Payne paper [11] needed to be made. This amendment allowed the ice height to increase as the glacier receded along an upward slope. This is required so that the otation criterion is continued to be met, however the experiments in the Vieli and Payne paper did not exhibit this behaviour. Despite this change in the behaviour of the ice height we still found that the retreat of the grounding line was stable for an upsloping bed, contradicting the results of Hindmarsh [3] and [7]. However the grounding line dynamics are more dependent on the basal topography than suggested in the Vieli and Payne paper [11].

In addition we have found that the tendency of the grounding line to advance or recede is dictated by the sign of the net accumulation. This is in contrast to the Vieli and Payne paper [11] where a small positive accumulation led to a receding grounding line. This is potentially caused by the moving mesh models in the Vieli and Payne paper not being locally mass conserving.

11.1 Further Work

11.1.1 Full Stokes Equations

Many numerical models make use of the shallow ice approximations. These approximations use vertical averaging to simplify the full Stokes' equations. There have been relatively few attempts to model the ice dynamics with the full Stokes' equations, but one example of a model using the full Stokes' equations occurs in the MISMIP paper. It was found there that the results of the full Stokes' equations yielded much larger changes to the grounding line position. This model is however computationally costly and modelling the grounding line with the use of full Stokes' equations includes the question of available computer resources.

11.1.2 Higher-Dimensions

(1(equate.2)-11e.2dyn(or9lp6ina.td57(er)-67(mes5(pap)-larg9n(o.793 764.48mensions)]TJ/F17 1

References

[1] Baines, M. J. , Hubbard, M. E. and Jimack, P. K., Velocity-based moving mesh methods for nonlinear partial di erential equations. Communications in Computational Physics, 10(3):509576 (2011)

[2] Goldberg, D., Holland, D. M. and Shoof, C., Grounding Line Movement and Ice Shelf Buttressing in Marine Ice Sheets, J Geophys. Res., Vol 114, doi:10.1029/2008JF001227 (2009)

[3] Hindmarsh, R.C.A, Stability of Ice Rises and uncoupled marine ice sheets, Ann. Glaciol., 23, 105-115 (1996)

[4] Partridge, D., Numerical Modelling of Glaciers: Moving Meshes and Data Assimilation, PhD Thesis, University of Reading, UK (2013)

[5] Pattyn, F., Schoof, C., Perichon, L., Hindmarsh, R. C. A., Bueler, E., de Fleurian, B., Durand, G., Gagliardini, O., Gladstone, R., Goldberg, D., Gudmundsson, G. H., Lee, V., Nick, F. M., Payne, A. J., Pollard, D., Rybak, O., Saito, F., and Vieli, A.: Results of the Marine Ice Sheet Model Intercomparison Project, MISMIP, The Cryosphere Discussion, Vol 6, 267-308, doi:10.5194/tcd-6-267-2012 (2012).

[6] Shepherd, A. and Wingham, A., Recent Sea-Level Contributions of the Antarctic and Greenland Ice Sheets, Science, 315, 1529-1532 (2007).

[7] Schoof, C., Marine ice-sheet dynamics. Part 1. The case of rapid sliding. Journal of Fluid Mechanics, 573:27 (2007)

[8] Thomas, R. Bentley, C. Model for Holocene retreat of the West Antarctic Ice Sheet. Quaternary Res, 10(2), pages 150-170.(1978)

[9] Van De27(cges)-32e2(G.)-b(De27l68G8(G.)-(C.,)-cVV)82(anTide[ena)(G.)-b1V[62,ana 17.3

[12] Weertman, J. Stability of the junction of an ice sheet and an ice shelf. J. Glaciol. Journel of Glaciology Vol. 13, 3-11, (1974)